

Diffusion and Reaction in Porous Glass

M. RAJA RAO and J. M. SMITH

University of California, Davis, California

Constant pressure diffusion rates of hydrogen through Vycor porous glass were measured in nitrogen and neon systems. The experimental diffusivities are less than those predicted by the random pore model indicating that this model may not be satisfactory for a low porosity material such as Vycor. Interpreted in terms of an assembly of parallel pores the data suggest a tortuosity factor of approximately 2.4.

Rate data for the ortho-para hydrogen reaction were also measured at -196°C. and 1 atm. The catalyst 2% nickel oxide/Vycor was found to have pore properties (area, mean pore size, pore volume) similar to that of plain Vycor. Predicted effectiveness factors using the experimental diffusion data were in good agreement with values determined experimentally. The latter were evaluated from rate measurements on both pellet and particles ($58\ \mu$ mean diameter).

The efficiency of a solid catalyst in converting reactants to products is dependent upon a high surface area per unit mass. This requires large numbers of small pore spaces distributed through the solid. The actual geometry of such pore spaces, as for example in alumina or silica gel, is complex enough to defy quantitative description. Hence it is necessary to employ more simply described models as representative of the pore structure. These idealized systems can be used to analyze the diffusion of reactants in the pores and so evaluate the effectiveness of the interior surface of a catalyst particle or pellet. A common model is to consider the pore structure as a series of uniform cylindrical capillaries that have a length kL that reflects the tortuous path through the solid phase. The pores are further assumed to be parallel rather than interconnected. More recently (13) a model of randomly interconnected capillaries has been used to describe how diffusion rates are related to the pellet density (and hence mean pore radius). A somewhat similar approach has been employed (15) to relate the diffusivities of several kinds of porous catalysts.

Extension of the random-pore theory to diffusion and reaction has given satisfactory results (9, 10, 14) for silica gel, and particularly alumina, catalysts. These materials are characterized by large pore volumes and, for alumina pellets, a broad pore size distribution. Vycor type of porous glass is a somewhat different material since it has a low porosity and contains a narrow distribution of rather small pores (see Figure 3). This combination of properties suggests fewer pore interconnections and therefore a structure that is closer to the parallel capillary model than the concept of randomly interconnected pores.

In this paper diffusion and reaction data, with a nickel oxide on Vycor catalyst, are used to analyze the two pore models. Diffusion measurements were made for the two

binary systems, hydrogen-nitrogen and hydrogen-neon, at 25°C. and 1 atm. total pressure. For combined diffusion and reaction processes the conversion of ortho to para hydrogen was studied at liquid nitrogen temperature (-196°C.) and 1 atm. pressure. All the measurements were made at steady state conditions.

To discuss diffusion in small pores it is necessary to have adequate data on the geometry of the porous solid. The pore volume, density, surface area, and volume pore-size distribution were evaluated by standard techniques for the Vycor and the nickel oxide/Vycor catalyst.

EXPERIMENTAL METHODS

Diffusion

Diffusion rates of hydrogen were measured at constant pressure in the apparatus shown in Figure 1. One end face of the Vycor cylinder was exposed to a moving stream of nitrogen (or neon) and the other to a stream of hydrogen. The hydrogen diffusing through the pores and into the nitrogen stream is analyzed in a thermal conductivity cell. The method has been described in detail by others (4, 16).

The cylinders were cut from rods (0.56-in. diameter) of Vycor. For studies on pure Vycor the cylinders, $\frac{1}{4}$ in. in length, were heated for 2 hr. at a temperature of 450°C. to remove water and then mounted in slightly undersized Tygon tubing, as shown in the detail sketch in Figure 1. The nickel oxide on Vycor catalyst cylinders were $\frac{1}{2}$ in. in length and had been heated at 450°C. in their preparation so that additional heat treatment prior to diffusion measurements was unnecessary. The purity of the nitrogen and hydrogen gases as supplied was 99.9% and 99.7%, respectively. However the hydrogen was further purified in a Deoxo unit (see Figure 1). The diffusion cell was at approximately 25°C. and at atmospheric pressure. The thermal conductivity cell was operated at a constant current of 125 milliamperes and inserted in a constant temperature bath at 25°C.

Reaction

The apparatus used for measuring the rate of the ortho-para hydrogen conversion at -196°C. and 1 atm. is shown in Figure 2. The reactant gas was electrolytic grade, normal hydrogen (hydrogen containing the equilibrium content of the para form at 25°C. , that is 25.0%). The conversion was measured by comparing the product composition with that of the feed in a thermal conductivity cell in accordance with the method of Weitzel and White (17). Care was taken to have the same flow rates of reactant and product streams through the cell. The cell was calibrated by determining the electromotive force when the product stream contained the equilibrium composition of para hydrogen at -196°C. This is 50.26% (20). Equilibrium was achieved by operating the reactor (U tube type shown in detail sketch of Figure 2) at successively lower flow rates until the product composition showed no further change.

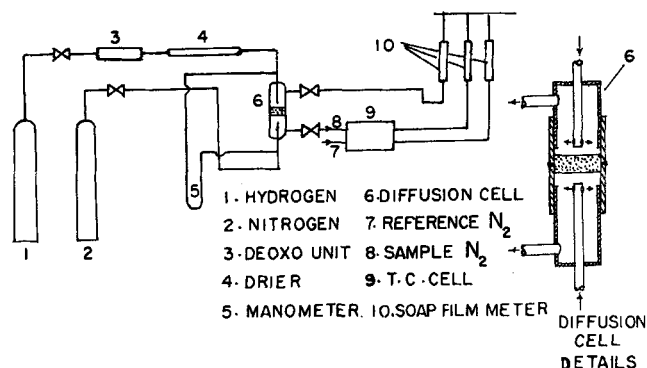


Fig. 1. Schematic flow diagram of diffusion apparatus.

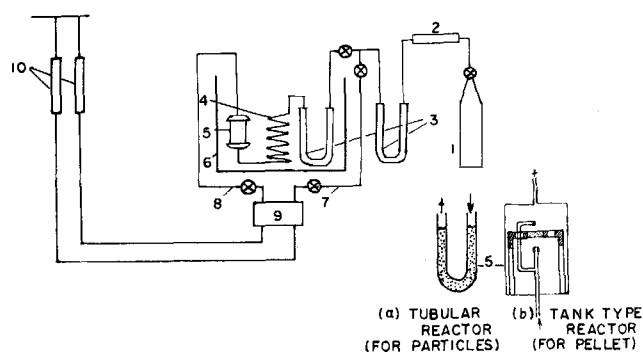


Fig. 2. Schematic flow diagram of reaction apparatus. 1. electrolytic hydrogen cylinder, 2. deoxo unit, 3. silica gel tubes, 4. pre-cooler, 5a. tubular reactor, 5b. tank type of reactor, 6. liquid nitrogen bath, 7. reference gas, 8. sample gas, 9. thermal conductivity cell, 10. soap-film meters.

Gas mixtures of intermediate composition for calibration points were obtained by mixing normal hydrogen with that at equilibrium at -196°C .

The apparatus and operating procedure for the kinetic measurements were similar to those described in the earlier work (10) except for the pellet reactor. The small diffusion rates in the low-porosity Vycor make it difficult to prevent leakage between pellet and container surfaces. Hence the technique used for alumina pellets, in which only one end face of the cylindrical pellet is exposed to the reacting gas, could not be employed. Instead a reactor was used in which both faces of the Vycor cylinder were exposed to the same reaction gas. The pellet was held in the reactor by cementing the lateral surface to the holder as shown in the detail sketch in Figure 2. The reactant stream was split sending part to one face and the remainder to the other. Tangential flow of the gas on either side of the pellet ensured stirred-tank reactor behavior.

After the kinetic measurements on the pellets were completed, they were ground to particles having an average diameter of $58\ \mu$. Rate data were then obtained for these particles in a U tube glass reactor ($\frac{1}{2}$ -in. I.D., 5 in. long), also shown in Figure 2. About 0.5 g. of catalyst particles were supported on glass wool in the tube to give a fixed bed, flow reactor. These data are necessary in order to obtain an experimental effectiveness factor by comparison with the rate data for the pellets.

Catalyst Preparation

A single batch of 2.0 wt. % nickel oxide/Vycor catalyst was prepared by evacuating $\frac{1}{8}$ in. long cylinders of Vycor at $150\text{-}\mu$ pressure for 6 hr. and then soaking in nickel nitrate solution at room temperature. To fit the reactor (Figure 2) the original cylinders (0.56-in. diameter) were ground, before impregnation, to a diameter of 0.50 in. The impregnated cylinders were dried at 110°C . for 2 hr. and then heated at 450°C . for 4 hr. to decompose the nitrate to nickel oxide. The decomposition

temperature at atmospheric pressure is about 400°C . (7). These pellets were used without further treatment for the kinetic measurements. Visual observation of fractured pellets showed a uniform grey-black color.

Preliminary runs with the empty U tube reactor and one packed with plain Vycor particles showed no activity for ortho hydrogen conversion.

Physical Properties of Vycor and Catalyst

A Sorptometer was employed to measure the adsorption equilibrium curves for Vycor and the nickel oxide/Vycor catalyst. This device determines the amount of adsorbed gas by concentration measurements in a continuous flow, constant pressure system. A mixture of helium and nitrogen of known composition is passed through the ground particles of the sample (previously degassed by heating in a stream of helium at 350°C . for 4 hr). The thermal conductivity of the mixture is monitored, with thermal conductivity cells placed upstream and downstream from the sample, and recorded. Initially the sample is cooled to -196°C ., and a certain amount of nitrogen is adsorbed. This adsorption is indicated by a peak on the strip-chart recorder. After adsorption equilibrium is established, the coolant is removed, and desorption of the nitrogen occurs as the sample returns to room temperature. The increase in nitrogen concentration in the nitrogen-helium stream shows up on the strip chart as a second peak, equal in area but opposite in direction to the adsorption peak. Finally a known volume of nitrogen is introduced into the stream and this results in a calibration peak. The area under the desorption peak is compared with that of the calibration peak to give the equilibrium adsorption of nitrogen at a p/p_0 value corresponding to the original concentration of nitrogen in the helium stream. Other compositions are then studied until the complete adsorption equilibrium curve is obtained.

From these experiments pore volumes were obtained directly and pore size distributions were calculated from a modified form of the Kelvin equation, as described by Pierce (8). The distribution curves for Vycor and for the catalyst, shown in Figure 3, are rather symmetrical and indicate a narrow range of pore radii. Mean radii \bar{a}_i are necessary to evaluate Knudsen diffusion coefficients for hydrogen. Hence diffusion-average values of \bar{a}_i were calculated by the method given earlier (13). The result for plain Vycor (45Å) is a little higher than that for the catalyst (39Å). Calculations indicate that 2.0 wt. % nickel oxide would provide a monomolecular coverage of 12 to 33% of the surface of the Vycor. The range in coverage is due to the uncertainty about the effective surface covered by one adsorbed molecule of nickel oxide. In any event a coverage in this range seems sufficient to produce the difference in pore geometry between catalyst and plain Vycor. The results for pure Vycor are somewhat larger than reported by the manufacturer for Vycor, perhaps due to the heat treatment given both the Vycor and catalyst.

The density of the pellets was measured directly. Then the porosity was determined by multiplying the density by the pore volume. Finally the surface areas were calculated from the adsorption equilibrium curve by the Bennett-Emmett-Teller method.

All of these property results are given in Table 1. The specific quantities V_i and S_g are referred to a unit mass of solid measured after the heat treatment. It should be noted that the Vycor pellets contain only micropores, as in silica gel. However the porosity is only 0.30 while that in silica gel is closer to 0.5. Similarly the microporous alumina studied earlier (13) had a porosity of about 0.5.

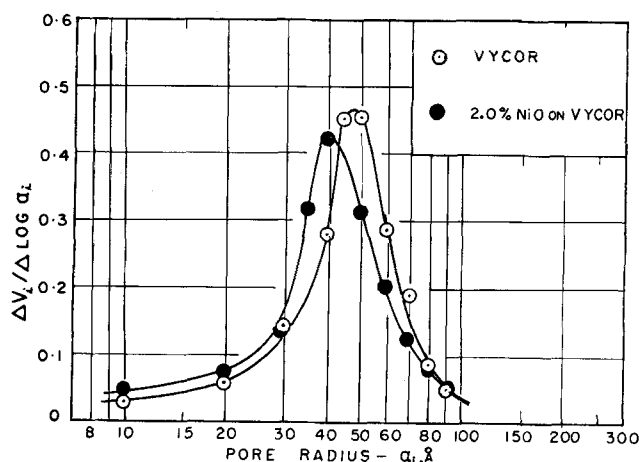


Fig. 3. Pore size distributions.

TABLE 1. PROPERTIES OF VYCOR AND CATALYST

	Density ρ , g./cc.	Pore volume, cc./g.	Micropore porosity, ϵ_i	Surface area S_g , sq. m./g.	Average pore radius \bar{a}_i , Å
Vycor	1.46	0.208	0.304	90	45
2.0% NiO on Vycor	1.47	0.210	0.314	107	39

TABLE 2. DIFFUSION DATA AND RESULTS FOR HYDROGEN (25°C., 1 ATM.)

A. Hydrogen-nitrogen system	Nitrogen flow rate range, cc./min.	Hydrogen diffusion rate, cc./min.	Effective diffusivity, sq. cm./sec.		
			Exp.	Predicted	
				Random pore model	Parallel pore model
Vycor pellet #1 (thickness ¼ in., mass 1.61 g.)	65-362	0.441	0.00293	0.00487	0.00245
Vycor pellet #2 (thickness ¼ in., mass 1.61 g.)	61-371	0.422	0.00282	0.00487	0.00224
2% NiO/Vycor #1 (thickness ½ in., mass 3.04 g.)	69-429	0.210	0.00280	0.00460	0.00245
2% NiO/Vycor #2 (thickness ½ in., mass 3.06 g.)	85-423	0.204	0.00272	0.00460	0.00224
B. Hydrogen-neon system					
Vycor pellet #3 (thickness ½ in., mass 3.36 g.)	57-100	0.192	0.00256	0.00487	0.00245
2% NiO/Vycor #2	86.5	0.185	0.00247	0.00460	0.00224

DIFFUSION RESULTS

Experimental Diffusivities

Diffusion rates were measured for two pellets of Vycor and two of catalyst with the hydrogen-nitrogen system. For each pellet data were obtained for a four to sixfold range of flow rates of nitrogen. The results, Table 2, show good agreement between runs at different flow rates. The data for different pellets is a better evaluation of the reproducibility of the measurements. The agreement in this case is 4% or better. Some results were also obtained for diffusion of hydrogen in the hydrogen-neon system for both plain Vycor and the 2.0% nickel oxide catalyst. The diffusivities (fourth column of Table 2) here were about 15% lower than for the hydrogen-nitrogen system for both Vycor and catalyst. This relatively small deviation indicates that surface diffusion of hydrogen is not large. More significant is the fact that Barrer and Barrie (1), from transient flow studies, found little evidence of surface diffusion for hydrogen on Vycor glass at room temperature. The results in Table 2 for plain Vycor agree well with the experimental data of Barrer and Barrie as noted later in discussing Table 3. Other investigations (3, 5, 6) of flow of gases through Vycor have also shown no surface diffusion for hydrogen at room temperature.

The effective diffusivities D_e were calculated from Fick's law, Equation (1). Note that this expression is

valid, that is D_e is independent of composition in the pellet, because the diffusion is predominantly of the Knudsen type in the small pores of Vycor. In terms of the molal diffusion rate N_H , the total cross-sectional area of the pellet A , and its length L , D_e is defined by the expression

$$D_e = \frac{N_H}{\Delta C_H} \left(\frac{L}{A} \right) \quad (1)$$

where ΔC_H is the difference in concentration of hydrogen across the two faces of the pellet. Using the measured volumetric diffusion rate V_H , and the partial pressure difference of hydrogen across the length of the pellet, one may write Equation (1) as

$$D_e = \frac{P V_H}{\Delta P_H} \left(\frac{L}{A} \right) \quad (2)$$

Owing to the small diffusion rate through Vycor ΔP_H was essentially equal to the total pressure P . The diffusivities given in Table 2 were calculated from Equation (2) with the average diffusion rates given in the same table.

Predicted Diffusivities—Random Pore Model

This model was developed (13) for catalyst pellets containing macropores (100 to 10,000 Å) surrounding microporous particles. It has been found to predict accurately diffusion rates for alumina pellets of different densities. In terms of the macro and micropore properties the effective diffusivity is given by the expression

$$D_e = \frac{\epsilon_a^2}{\frac{1 - \alpha_y}{D_b} + \frac{1}{\bar{D}_{ka}}} + \frac{\epsilon_i^2(1 + 3\epsilon_a)}{(1 - \epsilon_a)} \frac{1}{\frac{1 - \alpha_y}{D_b} + \frac{1}{\bar{D}_{ki}}} \quad (3)$$

The model can be applied to microporous materials by taking $\epsilon_a = 0$. For Vycor it is also true that the bulk diffusivity D_b is much greater than the Knudsen diffusivity. Then Equation (3) reduces to the simple form

$$D_e = \bar{D}_{ki} \epsilon_i^2 \quad (4)$$

This expression can be used to predict D_e without experimental diffusion data. However ϵ_i and \bar{a}_i are needed, the latter in order to calculate the mean Knudsen diffusivity from the equation

$$\bar{D}_{ki} = \frac{2}{3} \bar{a}_i \bar{v}_H \quad (5)$$

The last column of Table 3 shows that the values of D_e calculated in this way are about twice as large as the experimental results.

Predicted Diffusivities—Parallel Pore Model

In this model the pores are supposed to have an equivalent straight length of kL where k is the tortuosity factor. If there are n such pores per unit cross-sectional area of pellet, the diffusion flux N_H/A is given by

TABLE 3. RATE DATA (−196°C., 1 ATM.)

Catalyst	Flow rate, cc./sec. (25°C., 1 atm.)	Exit mole fraction, y_2	$W/F \times 10^{-5}$, (g. mole/) (g. mole/) (sec.)	$(k_w E_i) \times 10^6$, (g. mole/) (sec.)
A. Catalyst particles (average diameter = 58μ)				
2.0% NiO/Vycor (0.509g.)	3.08	0.297	0.0403	5.14
	2.47	0.306	0.0502	4.97
	1.98	0.321	0.0627	5.22
	1.48	0.340	0.0839	5.27
	1.27	0.356	0.0976	5.54
	1.08	0.365	0.115	5.26
	1.04	0.373	0.119	5.62
			Average	5.29
B. Catalyst pellets (½ in. diameter cylinders, approx. ⅓ in. in length)				
2.0% NiO/Vycor pellet #3 (0.521g.)	3.13	0.271	0.0413	($k_w E_i$) E_a 2.15
	2.50	0.277	0.0516	2.32
	2.04	0.281	0.0633	2.21
	1.48	0.290	0.0874	2.12
	1.27	0.294	0.102	2.08
	1.08	0.302	0.109	2.18
			Average	2.18
2.0% NiO/Vycor pellet #4 (0.545g.)	3.08	0.270	0.0432	1.95
	2.44	0.275	0.0545	1.99
	1.98	0.280	0.0672	2.02
	1.52	0.289	0.0876	2.09
	1.39	0.293	0.0960	2.12
	1.02	0.302	0.130	2.00
			Average	2.03

$$\frac{N_H}{A} = \frac{n(\pi a_i^2) \bar{D}_{ki} (\Delta C_H)}{k L} \quad (6)$$

The porosity, in accordance with the model, is

$$\epsilon_i = \frac{n(\pi a_i^2 L k)}{(1)L} = \pi \bar{a}_i^2 k \quad (7)$$

Combining Equations (6) and (7) one gets

$$N_H = \frac{A \epsilon_i}{k^2 L} \bar{D}_{ki} (\Delta C_H) \quad (8)$$

The expression for D_e for this model is then obtained by comparing Equations (1) and (8); that is

$$D_e = \frac{\epsilon_i \bar{D}_{ki}}{k^2} \quad (9)$$

Theoretical means of evaluating the tortuosity factor are not available. Hence the use of this model requires flow or diffusion data to determine k . The value of $\sqrt{2}$ has been proposed for k for porous materials. However from flow data Barrer and Barrie (1) have found 2.56 for a Vycor porous glass of similar pore sizes to that used in the present study. With this result D_e values were computed from Equation (9) and compared with the experimental results in Table 2. The agreement is good, particularly with the hydrogen-neon system. The same value of k was assumed to apply for the catalyst, and here again the predicted and experimental results for D_e agree well.

In summary, for Vycor with its combination of low porosity and small pores the random pore model predicts diffusion rates that are too high. The parallel, but tortuous, pore model appears to represent better the diffusion data. However this latter model includes a constant that must be evaluated experimentally. Hence all that can be said with confidence is that the experimental measurements of Barrer and Barrie agree with those reported here. It is to be noted in this connection that flow and diffusion measurements for Vycor are equivalent, since the diffusion is of the Knudsen type.

It would be useful to determine tortuosity factors for other microporous solids to see if their values could be related to that for Vycor through easily determined properties. If such were the situation, the tortuous pore model might be considered more suitable for micropores, while the random pore approach would be more suitable for macropore and macro, micropore systems.

REACTION RESULTS

The kinetic data obtained for the catalyst particles and pellets determine an experimental effectiveness factor E_a for the pellets. These results can be compared with estimates of E_a based upon diffusivity data. To accomplish this it is necessary first to calculate specific reaction rates for the catalyst particles. Measurements by Wakao et al. (11, 12) have shown that rate data for the ortho hydrogen conversion on nickel oxide can be correlated by a first-order reversible rate equation:

$$r_p = k_w E_i (y_e - y) \quad (10)$$

In this equation E_i is the effectiveness factor for the catalyst particle and k_w is the rate constant at 1 atm. pressure. The external diffusion resistance for particles larger than 58μ has been shown (12) to be negligible for catalysts of higher activity than nickel oxide. Hence the y in Equation (10) can be taken as the bulk gas phase composition rather than that at the particle surface. Combining Equation (10) with a mass balance of para hydrogen for a fixed bed flow reactor and integrating one obtains an expression for $k_w E_i$:

$$k_w E_i = \frac{1}{W/F} \ln \frac{y_e - y_1}{y_e - y_2} \quad (11)$$

Here y_1 and y_2 are the mole fractions of para hydrogen at the inlet and exit of the catalyst bed. Since the heat of reaction is very small, the constant temperature assumption inherent in Equation (11) is valid.

From the measured quantities $k_w E_i$ can be evaluated from Equation (11). The pertinent data and results are given in Table 3A. The micropore effectiveness factor can be estimated from the Wheeler development (18, 19) for spherical particles:

$$E_i = 3 \frac{h_i \coth h_i - 1}{h_i^2} \quad (12)$$

$$h_i = x_p \left(\frac{k_w \rho R T}{D_e P} \right)^{1/2} \quad (13)$$

From the experimental value for D_e given in Table 2 for the hydrogen-neon system and the product $k_w E_i$, given in Table 3, Equations (12) and (13) were solved for E_i and k_w . Because the particles are small ($x_p = 58/2 = 29 \mu$) the value of h_i is about 0.10. Under these circumstances E_i is essentially unity. This same result is obtained from the diffusivity data for the hydrogen-nitrogen system. Hence it may be concluded that the effectiveness factor for the particles of catalyst is unity and the values for $k_w E_i$ in Table 3 may be regarded as specific reaction rates.

Pellet Effectiveness Factors

In the stirred-tank type of reactor used for the pellets the rate is constant and related to the compositions entering and leaving the system by the expression

$$\bar{r} W = F (y_2 - y_1) \quad (14)$$

If the pellet effectiveness factor is E_a , the rate is also given by

$$\bar{r} = (k_w E_i) E_a (y_e - y_2) \quad (15)$$

since the well-mixed composition, to which the faces of the pellet are exposed, is y_2 . Combining Equations (14) and (15) one gets

$$(k_w E_i) E_a = \frac{F}{W} \frac{(y_2 - y_1)}{(y_e - y_2)} \quad (16)$$

The measured flow rates and compositions were used in Equation (16) to calculate $(k_w E_i) E_a$ for the pellets. Measurements were made as a function of flow rate for two different pellets, and the results are shown in Table 3B.

The ratio of $(k_w E_i) E_a$ and $k_w E_i$ from Table 3 gives experimental values for the pellet effectiveness factor E_a . Results based upon average values are given in the last column of Table 4. For comparison, predicted results for E_a can be obtained from $(k_w E_i)$ and the measured or calculated diffusivities reported in Table 2. Wakao (14) has presented the method of approach for a first-order, equal-molal, counterdiffusion case such as the ortho hydrogen conversion. The result, for one-dimensional diffusion (slab geometry) applicable to this catalyst pellet, consists of the equations

$$E_a = \frac{\tanh h_L}{h_L} \quad (17)$$

$$h_L = \frac{L}{2} \sqrt{\frac{(k_w E_i) \rho R T}{D_e P}} \quad (18)$$

In Equation (18) the pertinent length is one half the pellet length L since both sides are exposed to the gas.

TABLE 4. EXPERIMENTAL AND PREDICTED EFFECTIVENESS FACTORS

Experimental value	D_e ($-196^\circ\text{C}.$), sq. cm./sec.	Effectiveness factor, E_a Pre- dicted	Experi- mental
2.0% NiO/Vycor—pellet #3			0.41
2.0% NiO/Vycor—pellet #4			0.38
Predicted results			
Exp. diffusion ($\text{H}_2\text{-N}_2$ system)	0.00140	0.36	
Exp. diffusion ($\text{H}_2\text{-N}_2$ system)	0.00125	0.35	
Random pore model	0.00234	0.45	
Parallel pore model	0.00114	0.33	

To use Equation (18) the diffusivity at reaction temperature $-196^\circ\text{C}.$ must be estimated from the $25^\circ\text{C}.$ data given in Table 2. As mentioned earlier there appears from Barrer's data and others no evidence of surface diffusion for hydrogen at $25^\circ\text{C}.$ Since the boiling point of hydrogen is $57^\circ\text{C}.$ below $-196^\circ\text{C}.$, it will be supposed that at this temperature also the diffusion is entirely of the Knudsen type. Then the diffusivity is proportional to $T^{1/2}$, and the values of D_e given in Table 4 were calculated from those in Table 2 on this basis. With D_e and $(k_w E_i)$ known, Equations (17) and (18) were solved for E_a and reported as predicted values in Table 4.

The experimental values of E_a , 0.41 and 0.38, for the two pellets, are somewhat higher than the predicted result, 0.36, based upon experimental diffusivities. In view of the assumptions involved in extrapolating the $25^\circ\text{C}.$ diffusion data to $-196^\circ\text{C}.$, and in the formulation of the differential equations leading to Equations (17) and (18), this agreement is good. Actually the effectiveness factor is not very sensitive to changes in D_e . This is seen by comparison of the results obtained with the experimental diffusivity and those predicted by the random pore model. The diffusivities are 0.00140 and 0.00234 sq. cm./sec., respectively, but the effectiveness factors change but little, 0.36 to 0.45. This situation applies only for this particular reaction-diffusion system. For systems where E_a is higher variations in the diffusivity could be more significant.

ACKNOWLEDGMENT

The financial support of the National Science Foundation for this work is gratefully acknowledged.

NOTATION

A	= cross-sectional area of the pellet, sq.cm.
\bar{a}_i	= average radius of the micropores, cm.; \bar{a}_a = macropores
C_H	= concentration of hydrogen, g. moles/cc.; ΔC_H = concentration difference across the length of the pellet
D_b	= bulk diffusivity in the hydrogen-nitrogen (or neon) system, sq.cm./sec.
D_e	= effective diffusivity of hydrogen in the pellet, sq. cm./sec.
\bar{D}_{ka}	= average Knudsen diffusivity in the macropores, sq.cm./sec.
\bar{D}_{ki}	= average Knudsen diffusivity in the micropores, sq.cm./sec.
E_i	= effectiveness factor for the catalyst particle
E_a	= effectiveness factor for the catalyst pellet
F	= flow rate, g. moles/sec.
h_i	= Thiele modulus for catalyst particle (spherical) defined by Equation (13)
h_L	= Thiele modulus for catalyst pellet (slab geometry) defined by Equation (18)
k	= tortuosity factor in parallel pore model of pellet

k_w	= specific reaction rate, g. mole/(sec.) (g. of catalyst)
L	= length of cylindrical catalyst pellet, cm.
N_H	= rate of diffusion of hydrogen through the pellet, g. moles/sec.
n	= number of pores per unit cross-sectional area of pellet, according to parallel pore model
p_H	= partial pressure of hydrogen, atm.
P	= total pressure, atm.
r_p	= rate of reaction for the catalyst particle, g. moles of para hydrogen formed/(sec.) (g. catalyst)
\bar{r}	= average rate of reaction for the catalyst pellet, g. moles para hydrogen formed/(sec.) (g. of catalyst)
R	= gas constant, cc.(atm.)/(g. mole) ($^\circ\text{K}.$)
S_g	= surface area of porous solid, sq.cm./g.
T	= temperature, $^\circ\text{K}.$
\bar{v}_H	= mean velocity of hydrogen molecules, cm./sec.
V_i	= pore volume, cc./g. of porous solid
V_H	= volumetric diffusion rate of hydrogen, cc./sec.
W	= mass of catalyst, g.
x_p	= average radius of catalyst particles, cm.
y	= mole fraction para hydrogen; y_1 refers to stream entering reactor and y_2 to stream leaving reactor
y_e	= equilibrium value of para hydrogen at $-196^\circ\text{C}.$ (0.5026)
α	= $1 - N_B/N_A$, where N_B and N_A are the diffusion rates of the two components A and B; for equal molal counter diffusion $\alpha = 0$
ϵ	= porosity or void fraction; ϵ_a refers to macropores and ϵ_i to micropores
ρ	= density of catalyst pellet or particle, g./cc.

LITERATURE CITED

1. Barrer, R. M., and J. A. Barrie, *Proc. Roy. Soc.*, **213A**, 250 (1952).
2. Barrer, R. M., *J. Phys. Chem.*, **57**, 35 (1953).
3. Gilliland, E. R., R. F. Baddour, and J. L. Russell, *A.I.Ch.E. Journal*, **4**, 90 (1958).
4. Henry, J. P., B. Chennakesavan, and J. M. Smith, *ibid.*, **7**, 10 (1961).
5. Kammermeyer, Karl, *Chem. Eng. Progr. Symposium Ser. No. 24*, **55**, 115 (1959).
6. ———, and L. O. Rutz, *ibid.*, p. 163.
7. Kirk, R. E., and D. F. Othmer, ed., "Encyclopedia of Chemical Technology," Vol. 1, p. 641, Interscience, New York (1952).
8. Pierce, C., *J. Phys. Chem.*, **57**, 149 (1953).
9. Rao, M. Raja., N. Wakao, and J. M. Smith, "Diffusion and Reaction Rates for Ortho-Para Hydrogen Conversion," *Ind. Eng. Chem., (Fund.)*, to be published.
10. Rao, M. Raja., and J. M. Smith, *A.I.Ch.E. Journal*, **9**, No. 4, p. 485 (1963).
11. Wakao, N., P. W. Selwood, and J. M. Smith, *ibid.*, **8**, 478 (1962).
12. ———, *J. Catalysis*, **1**, 62 (1962).
13. Wakao, N., and J. M. Smith, *Chem. Eng. Sci.*, **17**, 825 (1962).
14. ———, "Diffusion and Reaction Rates for Porous Catalysts," *Ind. Eng. Chem. (Fund.)*, to be published.
15. Weisz, P. B., and A. B. Schwartz, *J. Catalysis*, **1**, 399 (1962).
16. Wicke, E., and R. Kallenbach, *Kolloid Z.*, **97**, 135 (1941).
17. Weitzel, D. H., and L. E. White, *Rev. Sci. Instr.*, **26**, 290 (1955).
18. Wheeler, Ahlborn, "Advances in Catalysis," Vol. 3, p. 250, Academic Press, New York (1950).
19. ———, "Catalysis," Vol. 2, p. 105, Reinhold, New York (1955).
20. Woolley, H. W., R. B. Scott, and F. G. Brickwedde, *J. Res. Nat'l. Bureau of Standards*, **41**, 379 (1948).

Manuscript received March 8, 1963; revision received August 12, 1963; paper accepted August 14, 1963.